PRICES SUBJECT TO CHANGE

PB 194 588

AIRCRAFT MICROWAVE MEASUREMENTS OF THE ARCTIC ICE PACK

Alan E. Strong, et al

National Environmental Satellite Center
Washington, D. C.

August 1970

NATIONAL TECHNICAL INFORMATION SERVICE

Distributed . . . 'to foster, serve and promote the nation's economic development and technological advancement.'

U.S. DEPARTMENT OF COMMERCE

This document has been approved for public release and sale.

Pam:53.087.23 STR

POLAR
PAM
1578

POLARPAM

ESSA NESCTM 25

PB194588

A UNITED STATES
DEPARTMENT OF
COMMERCE
PUBLICATION

ESSA Technical Memorandum NESCTM 25

U.S. DEPARTMENT OF COMMERCE
ENVIRONMENTAL SCIENCE SERVICES ADMINISTRATION
National Environmental Satellite Center

Aircraft Microwave Measurements of the Arctic Ice Pack

ALAN E. STRONG AND MICHAEL H. FLEMING

Reproduced by
NATIONAL TECHNICAL
INFORMATION SERVICE
U S Department of Commerce
Springfield VA 22151

WASHINGTON D.C.
August 1970

BOREAL INSTITUTE
LIBRARY
Rec'd: APR 1 1975 17752
Order No.
Price $5.75
Acc. No UTIS

ESSA TECHNICAL MEMORANDA
National Environmental Satellite Center Series

The National Environmental Satellite Center is responsible for the establishment and operation of the National Operational Meteorological Satellite System and the environmental satellite systems of the Environmental Science Services Administration. The three principal offices of NESC are Operations, System Engineering, and Research. ESSA Technical Memoranda facilitate rapid distribution of material which may be preliminary in nature and which may be published formally elsewhere at a later date.

Memoranda in the NESCTM series are available from the Clearinghouse for Federal Scientific and Technical Information, U.S. Department of Commerce, Sills Bldg., 5285 Port Royal Road, Springfield, Va. 22151. Price: $3.00 hard copy; $0.65 microfiche. Order by accession number shown in parentheses at end of each entry.

NESCTM 1 Publications by Staff Members, National Environmental Satellite Center and Final Reports on Contracts and Grants Sponsored by the National Environmental Satellite Center 1958-1966, March 1967. (PB-174 606)

NESCTM 2 Publications by Staff Members, National Environmental Satellite Center and Final Reports on Contracts and Grants Sponsored by the National Environmental Satellite Center 1967. January 1968. (PB-177 189)

NESCTM 3 Computer Processing of Satellite Cloud Pictures. C. L. Bristor, April 1968. (PB-178 319)

NESCTM 4 Modification of the APT Ground Station Recorder for Increasing the Size of Recorded DRIR Data. Arthur S. Vossler, May 1968. (PB-179 322)

NESCTM 5 NESC Digital Formatting System (DFS). Randall G. Hill, October 1968. (PB-180 588)

NESCTM 6 Computer Processing of TOS Attitude Data. J. F. Gross, November 1968. (PB-182 125)

NESCTM 7 The Improved TIROS Operational Satellite. Edward G. Albert, August 1968. (PB-180 766)
Supplement No. 1. Characteristics of Direct Scanning Radiometer Data, Edward G. Albert, April 1969. (PB-183 965)

NESCTM 8 Operational Utilization of Upper Tropospheric Wind Estimates Based on Meteorological Satellite Photographs. Gilbert Jager, Walton A. Follansbee, and Vincent J. Oliver, October 1968. (PB-180 293)

NESCTM 9 Meso-Scale Archive and Products of Digitized Video Data From ESSA Satellites. Arthur L. Booth and V. Ray Taylor, October 1968. (PB-180 294)

NESCTM 10 Annotated Bibliography of Reports, Studies, and Investigations Relating to Satellite Hydrology. D. R. Baker, A. F. Flanders, and M. Fleming, June 1970.

(Continued on inside back cover)

U.S. DEPARTMENT OF COMMERCE
Environmental Science Services Administration
National Environmental Satellite Center

ESSA Technical Memorandum NESCTM 25

AIRCRAFT MICROWAVE MEASUREMENTS OF THE ARCTIC ICE PACK

Alan E. Strong and Michael H. Fleming

Washington, D.C.
August 1970

CONTENTS

Page

Abstract 1

I. Introduction 1

II. The Microwave Mission 2

III. Data and Results 4

IV. Conclusions 7

References 8

Figures 10

AIRCRAFT MICROWAVE MEASUREMENTS OF THE ARCTIC ICE PACK[1]

Alan E. Strong and Michael H. Fleming

ABSTRACT. Microwave radiometer data (19.3 GHz or 1.6 cm) taken from an aircraft mission over the Arctic Ocean near Point Barrow, Alaska, are examined. The microwave brightness temperatures corresponding to varying ice pack conditions are correlated with simultaneous photography and infrared radiation data. Microwave measurements of the surface taken both through and from beneath a stratus cloudcover are investigated for atmospheric attenuation and emission effects. The influence of clouds is greatest when viewing surfaces such as water, which appears cold at microwave frequencies because of its low emissivity. In general, cloudiness diminishes the capability of the 19.3-GHz radiometer to discriminate between ice and water. Polynya and other openings in the ice pack display a characteristic brightness temperature near 100° K when viewed through a cloud-free atmosphere, whereas they appear as much as 20-40° K warmer when clouds intervene between the surface and the radiometer.

I. INTRODUCTION

Recent aircraft overflights have demonstrated that remote sensing within the microwave region of the electromagnetic spectrum affords great promise of useful information to the oceanographer, meteorologist, hydrologist, geologist, geodesist, and geographer. The present Nimbus satellite schedule indicates that microwave data of Earth from the vantage point of space[2] will become available during 1972. At 19.35 GHz (1.6 cm), the microwave radiometer will be viewing Earth's surface close to the atmospheric water vapor attenuation peak (22.235 GHz). Although data presented in this study are from a radiometer nearly identical to the proposed Nimbus instrument, discussion will not be limited to this frequency. Background information on microwave radiometry is available from several sources (Paris 1969, Porter and Florence 1969, Edgerton et al. 1968, Hyatt 1967, and Shifrin 1968). Specific information on this 19.35-GHz passive system can be found in Nordberg et al. (1969),

---

1. Material in this Technical Memorandum was presented under the same title at the 51st Annual Meeting of the American Geophysical Union, Washington, D.C., 20-24 April 1970.
2. In 1968, the U.S.S.R. launched Cosmos 243 which carried a passive microwave sensor (4-38 GHz).

Stogryn (1967), and Catoe et al. (1967). Discussion of the radiometer specifics is not given here because the interested reader may refer to the above cited publications.

On May 31, 1967, NASA's Convair 990 flew over the Arctic Ocean from Point Barrow, Alaska. Figure 1 provides a chart of area and flight track. During this flight, data were gathered through clouds and from beneath the clouds over solid pack ice, open pack, young ice, open water, and snow. During early May of the same year some radar scatterometry data were taken by NASA. A report documenting these data was published recently by Rouse (1969). Comparisons between the two flights were not possible since the scatterometry mission was concerned with less variable ice conditions 150 miles north-northeast of Point Barrow and the radiometry mission with the more irregular ice concentrations within several tens of miles from Point Barrow.

II. THE MICROWAVE MISSION

Instruments on the Convair 990 pertinent to this report were: (1) the electrically scanning microwave radiometer, (2) a scanning medium-resolution infrared radiometer (MRIR), and (3) a 9- by 9-inch downward-looking camera. The 19.35-GHz radiometer scans from left to right beneath the aircraft. Data were obtained from 39 incremental steps from 50° left to 50° right of nadir. The field of view (FOV) at each step is 2.8°. Digitized and calibrated radiometric brightness temperatures were made available by NASA. Table 1 shows the effect of scan angle from nadir and of altitude on the dimensions of the radiometer's FOV at the Earth's surface. The 600-nautical-mile altitude included in this table provides a resolution comparison for the planned orbit of the Nimbus satellites. The scale of floe size categories is included to illustrate the instrument's ground resolution in terms of floe classification.

The MRIR scanned fore-to-aft beneath the aircraft along the flight path. Of the five channels of data available from the MRIR, the discussion is limited to the 10-11 micrometer window (channel 2). Surface temperatures are derived from these data when clouds are not present in the atmosphere between the instrument and the surface.

A rotating mirror in the MRIR provides a scan line every 7.5 seconds through a 2.9° aperature of the surface below (Cherrix and Sparkman 1967). Consequently, assuming that atmosphere attenuation can be accounted for, data at nadir from both the microwave and infrared radiometers provide surficial information from nearly equivalent scan-spot dimensions.

A T-11 camera with a 9- by 9-inch frame was used to take downward-looking, black and white photographs. The 74° by 74° field of view of this camera (Catoe et al. 1967) provided sufficient coverage to correlate with the radiometers.

Table 1.--Field of view for the 19.35 GHz microwave radiometer at various altitudes and scan angles.

Scan Angle from the Nadir	Altitude of Radiometer 0.3 Km. width length	10 Km. width length	1,110 Km. width length
0°	▨ 15 m X 15 m	▦ 489 m X 489 m	54 Km X 54 Km
10°	▨ 15 " X 15 "	▦ 504 " X 496 "	56 " X 55 "
20°	▨ 17 " X 16 "	▩ 554 " X 520 "	61 " X 58 "
30°	▨ 20 " X 17 "	▩ 652 " X 562 "	72 " X 63 "
40°	▥ 26 " X 19 "	▩ 833 " X 638 "	92 " X 71 "
50°	▥ 36 " X 23 "	▩ 1184 " X 760 "	131 " X 84 "

Ice Cakes	Small Floes	Medium Floes	Big Floes	Vast Floes	Giant Floes
▨ 2-20 m	▥ 20-100 m	▦ 100-500 m	▩ 500-2000 m	2-10 Km	>10 Km

The weather at Point Barrow during this flight (1200 LMT) included broken to overcast low stratus at the inversion ceiling (approximately 1 km and 0°C) and light snow. The shelter-level maximum daily air temperature had been about -5°C for the week prior to the flight and was -2°C at the time of the flight.

A high altitude run out from Point Barrow at 10 km provided microwave data of the water and ice that were partially contaminated with intervening cloud and atmosphere (to be discussed later). These effects were minimized on the return transit, because the plane flew beneath the stratus at an average altitude of 0.3 km (300 meters). The low-level pass was to have duplicated the track of the high-level pass, but the navigation data are not adequate to determine precisely the degree of error. The low-level flight, however, was well within the relatively wide swath covered by the high-level data. Photographic, microwave, and infrared data along the low-level pass thus can be compared with data from the high-level pass.

III. DATA AND RESULTS

The spectral intensity (I_o) of the radiation emitted, as viewed from the aircraft at an angle θ from nadir, is proportional to the absolute temperature (T_W) and emissivity (ϵ) of the viewed surface:

$$I(\theta) \approx \epsilon(\theta)\ T_W.$$

The intensity of radiation, regardless of angle, has been commonly referred to as brightness temperature (T_B):

$$T_B \approx \epsilon T_W.$$

Microwave brightness temperature values are available in a digitized mode from NASA at approximately 2.8° increments along every scan line. To stay within the limits of the photography (±37°), only the microwave data ±30° from nadir were used. Figure 2 shows the scanning of the microwave radiometer relative to the photography. Photographs were taken at a 10-second interval, whereas the microwave scanning was done at a 2-second interval during the high altitude pass and increased to 1-second intervals at low altitude. Consequently, at the speed the aircraft was flying (approximately 285 knots at the low altitude and 490 knots at the high altitude), neither the microwave imagery nor the photographs were contiguous.

A small time difference between the scanner and the camera was found during analysis. From several photographs showing abrupt

boundaries between ice (high emissivity) and water (low emissivity), a 2-second discrepancy was found to exist between these two systems. An adjustment has been incorporated into the data analysis and correlation without specifying which instrument was in error.

A test for signal homogeneity as a function of scan angle was made using selected portions of the low-level data pass taken over the ice-free water and over compacted pack ice (solid pack ice). The data locations were easily established from the photographic observations and from the rather uniform character of the mapped T_B values. Results are presented in figures 3 (open water) and 4 (pack ice). An average of 30 scan lines was used for the open water test; an average of 13 scan lines was used for the ice analysis. The microwave radiation over calm water follows the predicted near-cosine fall-off with increased angle from nadir (Stogryn 1967). The maximum variance of the observed brightness temperatures over water using both left and right scan angles was determined to be about 5°K. Over ice this variance was between 5°K and 10°K. Although quantitatively the extremely low T_B's indicated by the radiometer over water appear doubtful, one would expect calibrated values to be near 120°K (Paris 1969); the relative measurements are of interest. Brightness temperatures over ice, due to the remarkedly different roughness characteristics of ice opposed to water, display no marked decrease with increasing angle from nadir until greater than 30°. A recent U.S.S.R. report states that this property also is present at 10 GHz (Shifrin 1968).

It has been stated that the ice-water boundary is easily identified in the microwave imagery (NCMRED 1967). This is readily seen by comparing figures 3 and 4. Emissivities in the microwave region are near unity for ice, whereas water has been found to have an emissivity near 0.4. This large differential enables water and ice of equal thermal temperatures to be readily distinguished by means of microwave remote sensing.

If all ice produced a characteristic microwave brightness temperature around 250°K, one should be able to map ice concentrations per scan spot directly as a function of T_B. However, several other variables contribute to this observed T_B: (1) The surface thermal temperature may vary widely as a function of ice thickness (insulation) and during periods of radiative cooling; (2) the dielectric constant, intrinsically tied to salinity, is dependent largely on the age of the ice, since less salt characterizes older ice; and (3) moreover, thickness alone (at least the initial 4-5 meters of development) has been shown to markedly increase the microwave radiation (Shifrin 1968). Paris (1968) discusses many of these relationships.

Due to considerable signal "noise," it was necessary to subject the microwave data to an averaging process. With the much coarser resolution

from the high altitude pass compared with the lower one, it was necessary to perform different data manipulations at each altitude. Data from the 0.3-km pass were condensed into average values from two adjacent scan spots (three at nadir) from two successive scan lines. Data from nadir to ±30° were utilized. At the 10-km altitude full resolution data between ±10° were employed for analysis. Despite a reduced scan angle, the 10-km pass coverage perpendicular to the flight track is ten-fold that obtained during the 0.3-km pass. The analyses of the microwave data after rectification and together with the 0.3 km photography are presented in figures 5, 6, and 7. The horizontal (along flight line) scales are identical for both strips, whereas the vertical (normal to flight line) scales differ and are indicated. Even with this coarse analysis using 20°K intervals in T_B, the potential of microwave for depicting ice-water boundaries is apparent (fig. 7). Solid pack ice (fig. 7) and open water (figs. 5 and 6) show comparatively homogeneous temperature fields (240°K and 100°K, respectively), as opposed to close pack ice areas farther from shore (fig. 5). The regions intermediate in T_B to these extremes represent varied ice conditions, primarily where ice and water conglomerates are below the resolution of the scan spot averages or where very thin ice (gray ice) prevailed.

At the 10-km altitude the width of the field of view for the nadir position is 470 meters; at the 0.3-km altitude this width can be obtained by scanning ±38° from nadir. It was felt that the 0.3-km data should be restricted to ±10° from the nadir so that the information would not be overly obscured by more averaging. This swath width is 106 m. Since the higher flight was run at nearly twice the speed of the 0.3-km pass, all 0.3-km data within ±10° from nadir and over 4-second intervals have been averaged to match, as closely as possible, the nadir values obtained during the 10-km pass. Figure 8 presents this comparison. The cloud effects in the high altitude data seem particularly apparent, although the ice-water boundary is still dramatically apparent. An increase in cloud thickness away from shore is suggested. At 4.3 nautical miles from the ice-water boundary a big floe (fig. 5) is partially resolved by the ±10 swath average from 0.3 km. Clouds and the increased width of the 10-km swath obscure this feature. Immediately off the ice-water boundary the open water T_B from both altitudes is within 10-15°K. This differential increases to 40-60°K about 5 nautical miles from the ice-water boundary.

Several reports on studies made from Earth-based radiometers looking at the sky or sun suggest considerable allowance must be made for cloud and water vapor attenuation and emission (Haroules and Brown 1969). Kriess (1968) has presented theoretical results of liquid water effects on Earth T_B. His computations show that a 1-km thick stratus layer with a cloud top temperature of 277°K will increase the measured T_B by nearly 20°K at the nadir. In his calculations, he assumed the liquid content of the cloud to be 0.3 gm m^{-3}. It is doubtful that the stratus observed

in the case considered here had such a high liquid-water content. However, as shown by Porter (1970), an additional 10°K brightness temperature (over water) may easily be added by the intervening atmosphere through emissions from water vapor and gases. Several tens of degrees of brightness temperature are a customary stratus contribution.

A final analysis was performed comparing 0.3-km infrared and microwave data. The comparison is provided in figure 9. No infrared data exist for the 10-km pass. Due to the opposed scanning modes (discussed earlier), comparison was possible only at nadir. Registry of these data was obtained that corresponds to a 16-km path at nadir along the 0.3-km flight line. Considerable noise in the signal limited the benefit of this comparison. Nevertheless, it appears that little temperature difference existed between the ice and water surfaces. A differential would be expected only when the air temperature is well below the freezing temperature of the sea water (approximately -2°C).

IV. CONCLUSIONS

Microwave apparent brightness temperatures taken over ice and water indicate that a substantial contribution of additional microwave energy from stratus cannot be neglected. Over water, where emissivities are low, this effect is quite significant. At 19.35 GHz (1.6 cm), water vapor alone may significantly increase any horizontally polarized radiation over water. The 100-150°K range in T_B exhibited by ice provides a quantitative contrast. This contrast could enable satellite reconnaissance to provide additional information, such as thickness, salinity, and thermal temperature of the ice. If, however, variable atmospheric contamination is not held accountable, the range of ice T_B is decreased, and relative measurements may be all that are practicable. It is quite possible that lower microwave frequencies will recover more quantitative measurements of ice type and thickness.

As the observational frequency of microwave radiation is decreased, the antenna size must increase to maintain comparable ground resolution. One must constantly be aware of the limitations as to what can be resolved. Ice leads or polynyas readily visible from an aircraft microwave system may be well beyond the resolution capabilities of a similar system on an orbiting satellite. Furthermore, highly variable ice conditions below resolution capabilities appear at some intermediate T_B between the ice-free water and solid pack ice extremes. These intermediate T_B's are not necessarily unique because they also can be indicative of a fairly thin homogeneous or gray ice. Consequently, for ice surveillance coincident photography (high resolution) in addition to thermal imagery supplies excellent auxiliary inputs to a microwave radiometer system. Other potential supplementary information may be provided through dual polarization, active and passive (scatterometry) sensing, and multifrequency microwave imagery.

REFERENCES

Catoe, C., Nordberg, W., Thaddeus, P., and Long, G., "Preliminary Results from Aircraft Flights of an Electrically Scanning Microwave Radiometer," Report X-622-67-352, Goddard Space Flight Center, Greenbelt, Md., August 1967, 35 pp.

Cherrix, G. T. and Sparkman, B. A., "A Preliminary Report on Bidirectional Reflectances of Stratocumulus Clouds Measured with an Airborne Medium Resolution Radiometer," Report X-622-67-48, Goddard Space Flight Center, Greenbelt, Md., February 1967, 33 pp.

Edgerton, A. T., Mandl, R. M., Poe, G. A., and Jenkins, J. E., "Passive Microwave Measurements of Snow, Soils, and Snow-Ice-Water Systems," Technical Report No. 4, SGD 829-6, Contract NOnr 4767(00) NR 387-033, Aerojet-General Corp., El Monte, Calif., February 1968, 340 pp.

Haroules, G. G. and Brown, W. E., "The Simultaneous Investigation of Attenuation and Emission by the Earth's Atmosphere at Wavelengths from 4 Centimeters to 8 Millimeters," Journal of Geophysical Research, Vol. 74, No. 18, August 20, 1969, pp. 4453-4471.

Hyatt, H. A., "Analysis of Measurements of Microwave Emission from the Earth's Surface and Atmosphere," ESSA Contract No. E-43-67(N), DAC-60693, Douglas Missile and Space Systems Division, Douglas Aircraft Company, California, June 1967, 50 pp.

Kriess, W. T., "Meteorological Observations with Passive Microwave Systems," Boeing Scientific Research Laboratories Document D1-82-0692. Boeing Aircraft Company, Seattle, Wash., February 1968, 198 pp.

National Council on Marine Resources and Engineering Development, United States Activities in Spacecraft Oceanography, Washington, D.C., 1967, 44 pp.

Nordberg, W., Conaway, J., and Thaddeus, P., "Microwave Observations of Sea State from Aircraft," Quarterly Journal of the Royal Meteorological Society, Vol. 95, No. 404, 1969, pp. 408-413.

Paris, J. F., "Microwave Radiometry and Its Application to Marine Meteorology and Oceanography," Reference No. 69-IT, Office of Naval Research Contract NOnr 2119(04), Texas A&M University, January 1969, 210 pp.

Porter, R. A., "An Analysis of Airborne Microwave Radiometric Data," Final Report, Contract NAS 5-11685, Radiometric Technology, Inc., Cambridge, Mass., February 7, 1970, 116 pp.

Porter, R. A. and Florence, E. T., "A Feasibility Study of Microwave Radiometric Remote Sensing," NASA Contract No. NAS 12-629, Electronics Research Center, Cambridge, Mass., January 29, 1969, 294 pp.

Rouse, J. W., "Arctic Ice Type Identification by Radar," Proceedings of IEEE, Vol. 57, No. 4, April 1969, pp. 605-611.

Shifrin, K. S. (editor), Transfer of Microwave Radiation in the Atmosphere, Translation available from Clearinghouse for Federal Scientific and Technical Information, TT 69-55104, 1968, 160 pp.

Stogryn, A., "Apparent Temperatures of the Sea at Microwave Frequencies," IEEE Transactions on Antennas and Propagation, Vol. AP-15, No. 2, March 1967, pp. 278-286.

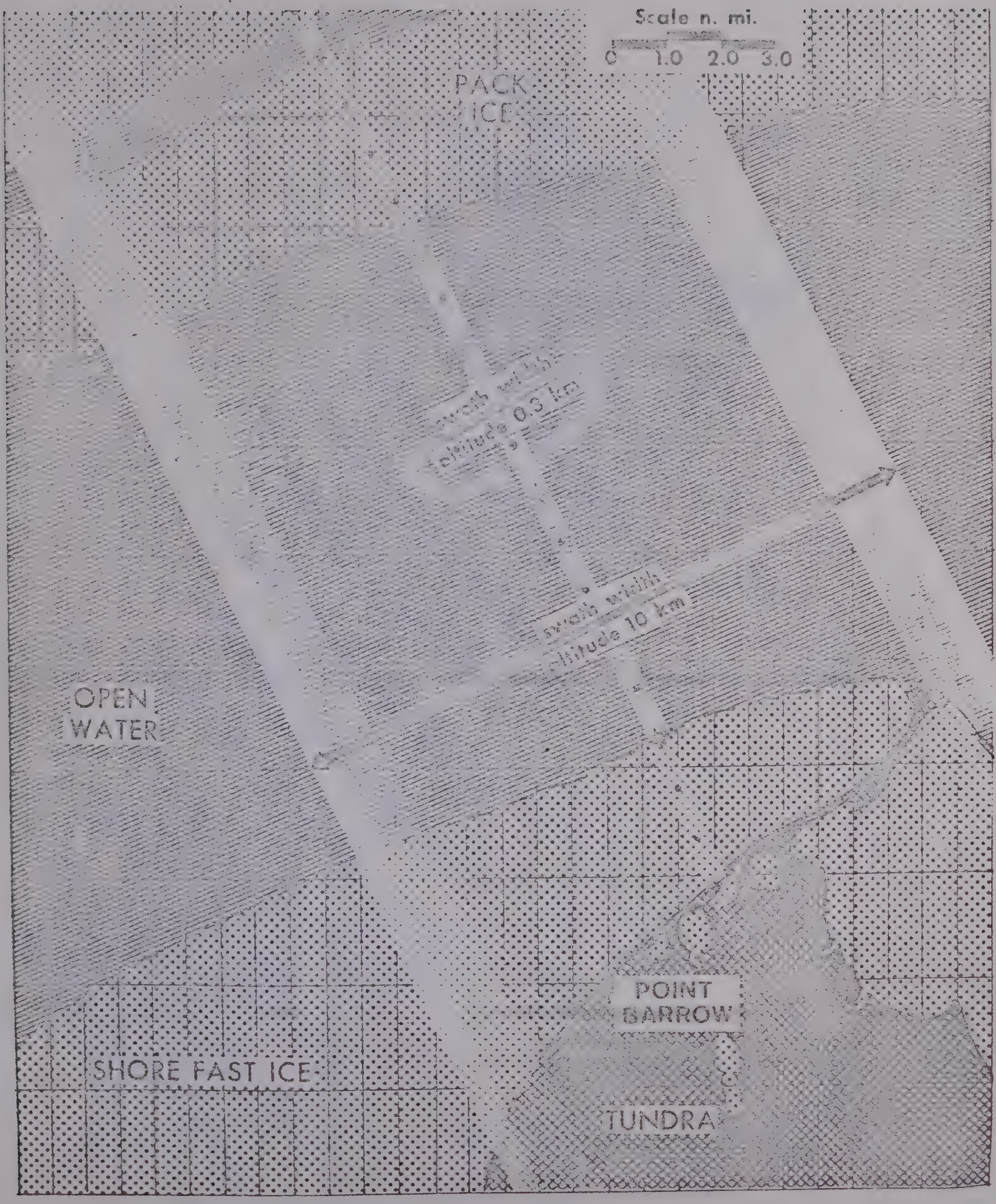

Figure 1.--Chart of Point Barrow, Alaska, showing the approximate ice boundaries.

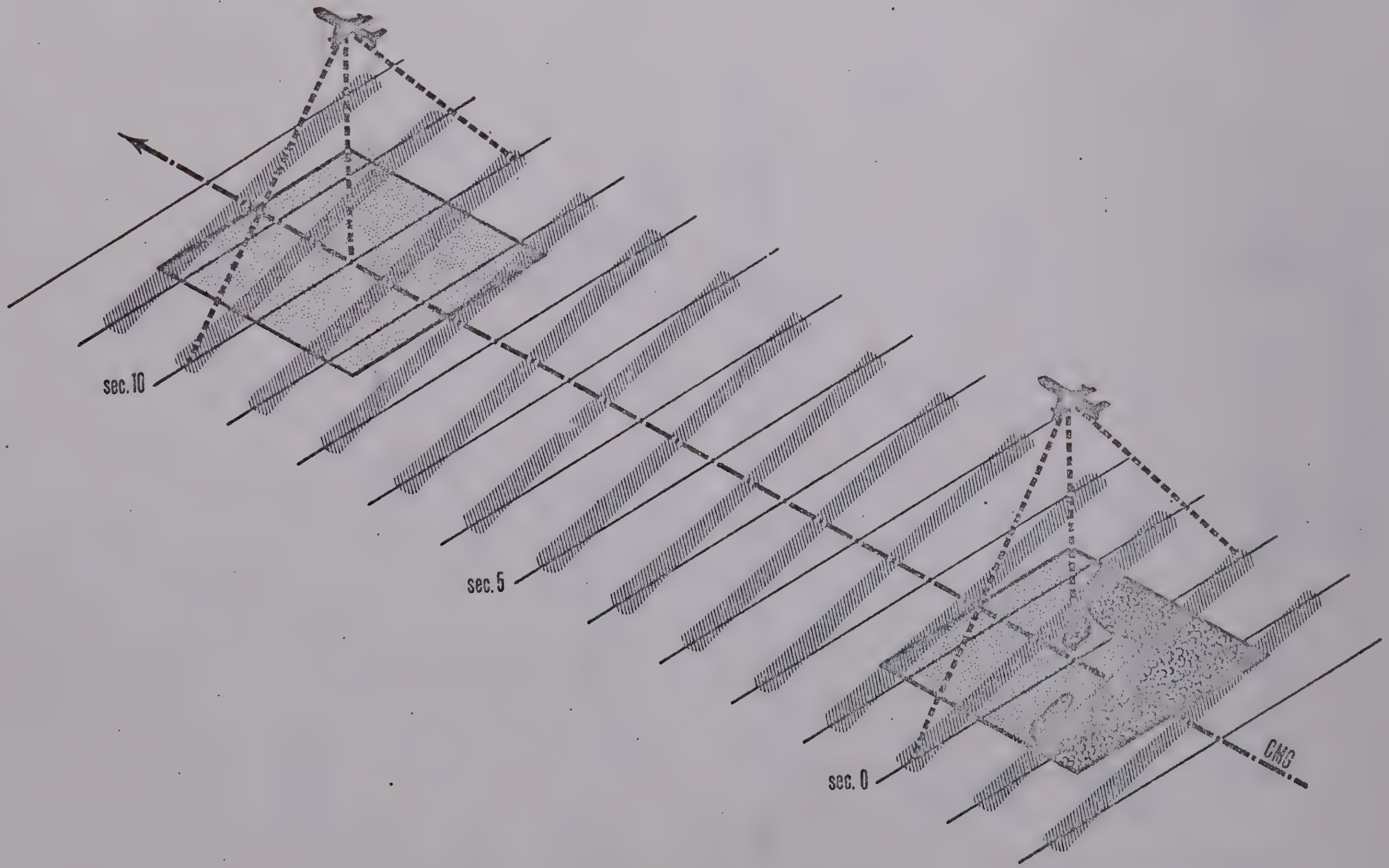

Figure 2.--Relationship of microwave radiometer swaths to ground truth photography.

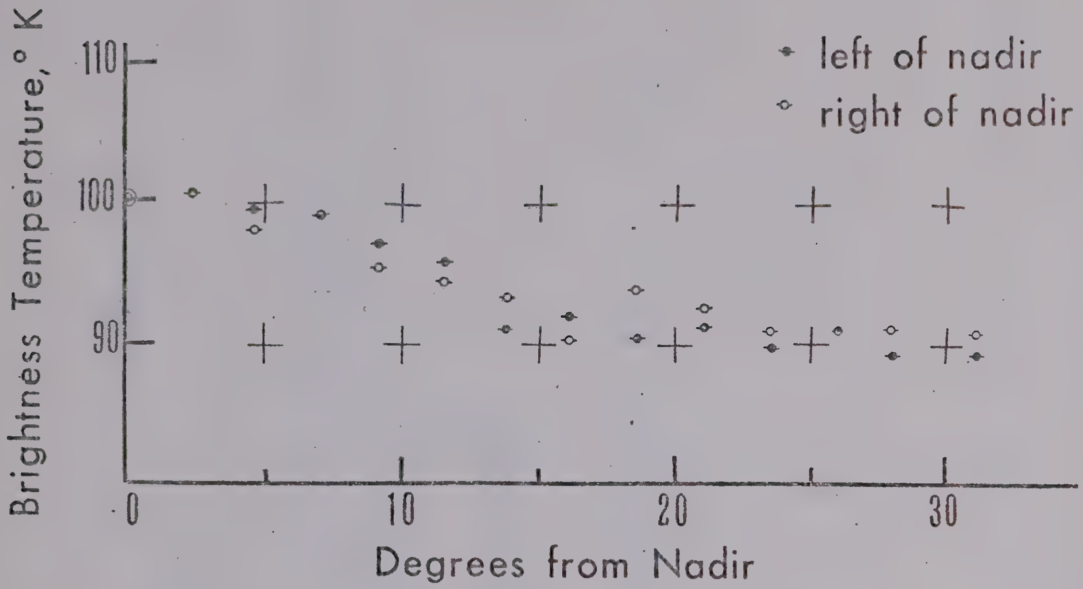

Figure 3.--Ice-free water microwave brightness temperature at selected scan angles.

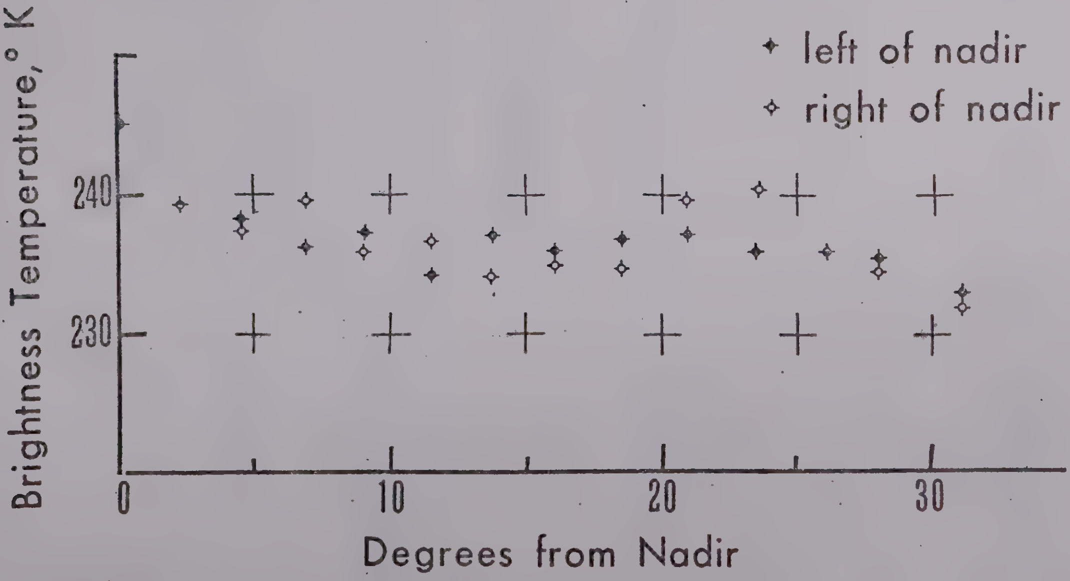

Figure 4.--Compact pack ice microwave brightness temperature at selected scan angles.

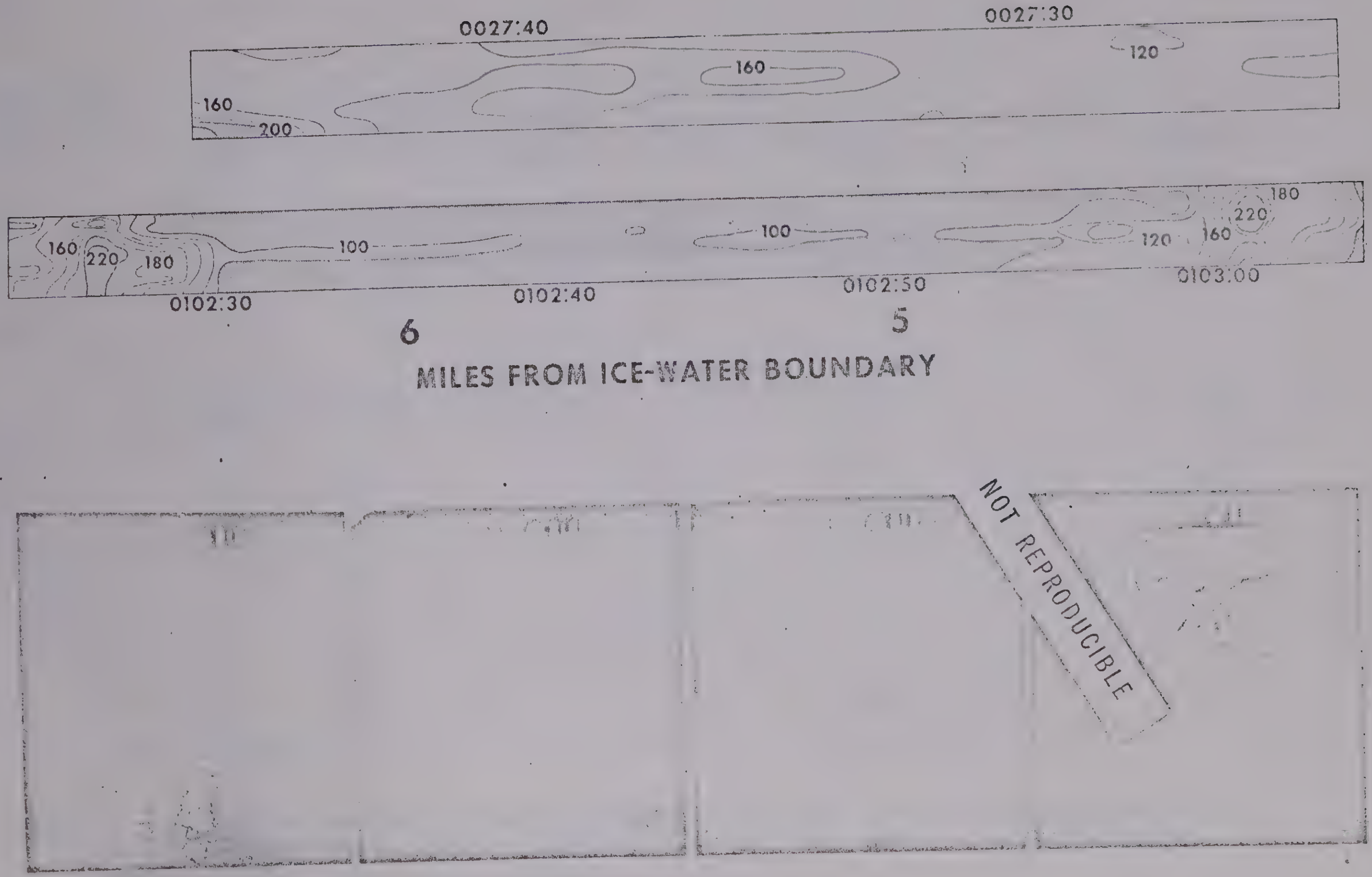

Figure 5.--Rectified microwave imagery from high (top) and low (middle) altitude with concurrent photography from low altitude 4 to 7 n. mi. from ice-water boundary. Imagery widths: top, 2 n. mi.; middle, 0.2 n. mi. Photographic dimensions: 0.25 x 0.25 n. mi. concurrent with low altitude imagery at mid-point of photograph.

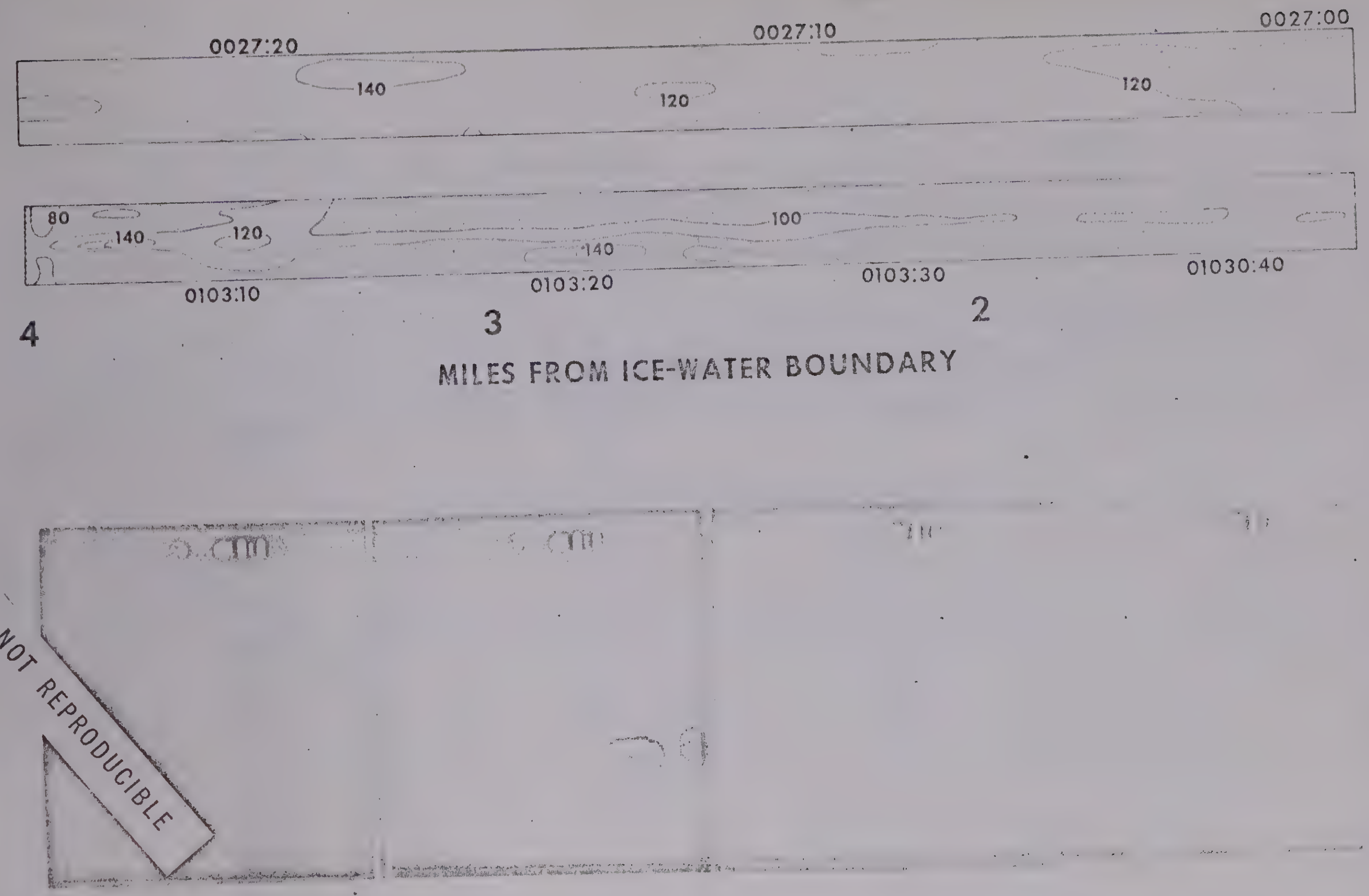

NOT REPRODUCIBLE

Figure 6.-- Rectified microwave imagery from high (top) and low (middle) altitude with concurrent photography from low altitude 1 to 4 n. mi. from ice-water boundary. Imagery widths: top, 2 n. mi.; middle, 0.2 n. mi. Photographic dimensions: 0.25 x 0.25 n. mi. concurrent with low altitude imagery at mid-point of photograph.

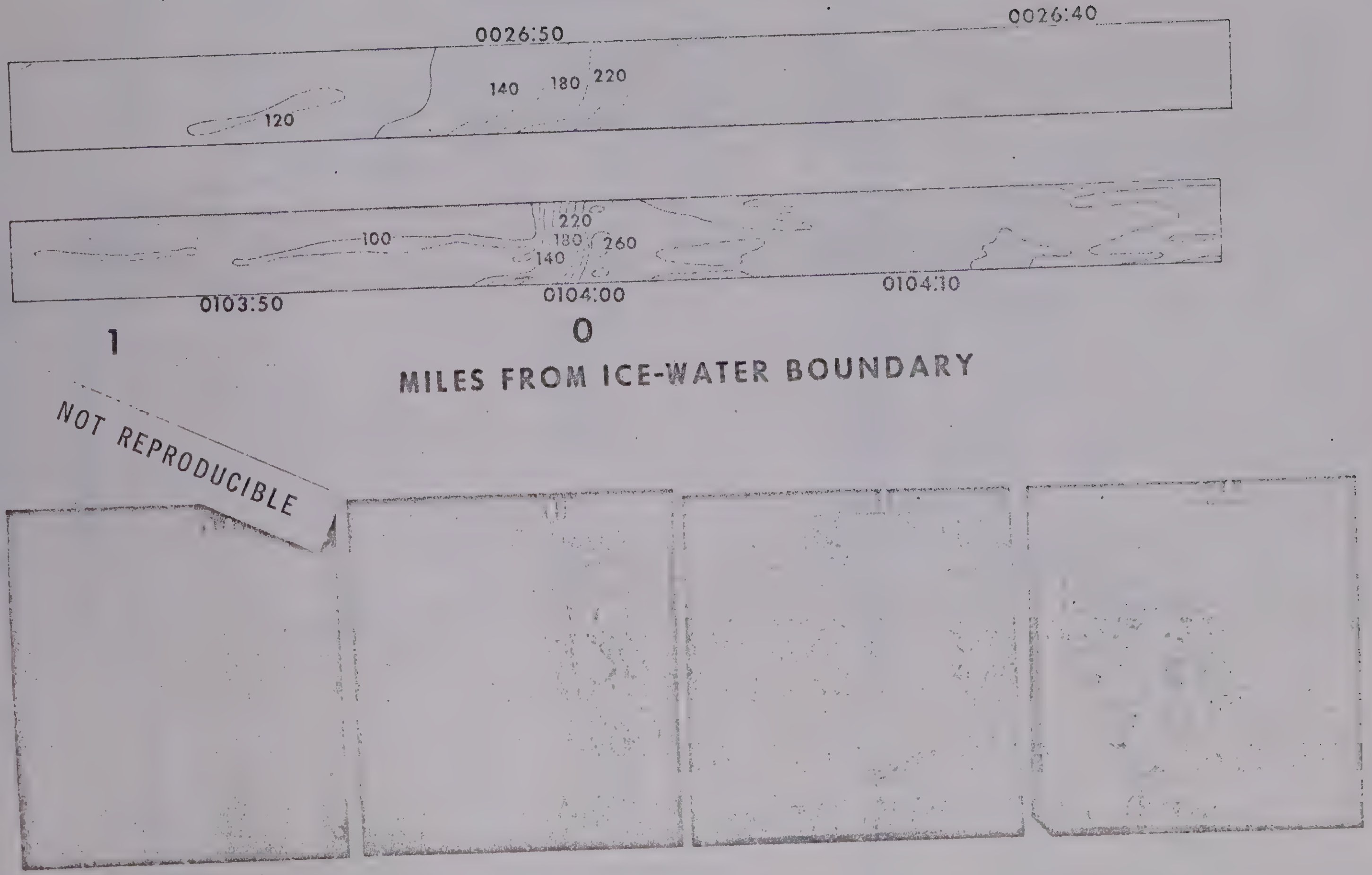

Figure 7.--Rectified microwave imagery from high (top) and low (middle) altitude with concurrent photography from low altitude at the ice-water boundary.
Imagery widths: top, 2 n. mi.; middle, 0.2 n. mi.
Photographic dimensions: 0.25 x 0.25 n. mi. concurrent with low altitude imagery at mid-point of photograph.

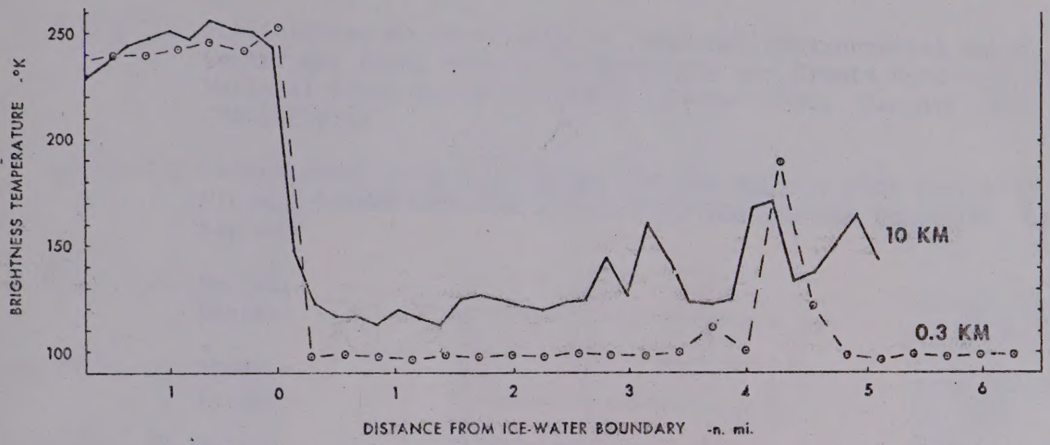

Figure 8.--Comparison of microwave brightness temperatures from the 10-km altitude pass and the 0.3-km altitude pass.

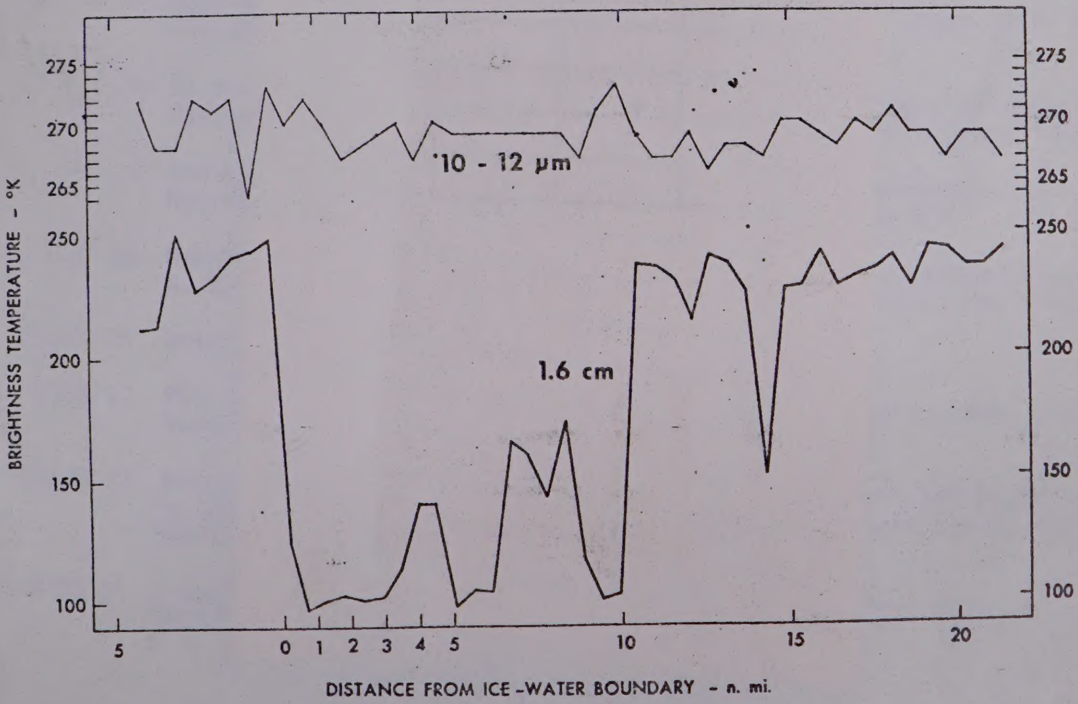

Figure 9.--Comparison of infrared and microwave data.

Date Due

17752

Pam:53.087.23
STR

AUTHOR
STRONG, Alan E. and FLEMING, Michael H.

TITLE
Aircraft microwave measurements...

DATE LOANED	BORROWER'S NAME	DATE DUE

Pam: 53.087.23 STR

STRONG, Alan E. and FLEMING, Michael H.

Aircraft microwave measurements of the Arctic ice pack. #17752

Boreal Institute for Northern Studies Library
CW 401 Bio Sci Bldg
The University of Alberta
Edmonton, AB Canada T6G 2E9

(Continued from inside front cover)

NESCTM 11 Publications by Staff Members, National Environmental Satellite Center and Final Reports on Contracts and Grants Sponsored by the National Environmental Satellite Center 1968. January 1969. (PB-182 853)

NESCTM 12 Experimental Large-Scale Snow and Ice Mapping With Composite Minimum Brightness Charts. E. Paul McClain and Donald R. Baker, September 1969. (PB-186 362)

NESCTM 13 Deriving Upper Tropospheric Winds by Computer From Single Image, Digital Satellite Data. Charles S. Novak, June 1969. (PB-185 086)

NESCTM 14 Study of the Use of Aerial and Satellite Photogrammetry for Surveys in Hydrology. Everett H. Ramey, March 1970. (PB-191 735)

NESCTM 15 Some Aspects of the Vorticity Structure Associated With Extratropical Cloud Systems. Harold J. Brodrick, Jr., May 1969. (PB-184 178)

NESCTM 16 The Improvement of Clear Column Radiance Determination With a Supplementary 3.8μ Window Channel. William L. Smith, July 1969. (PB-185 065)

NESCTM 17 Vidicon Data Limitations. Arthur Schwalb and James Gross, June 1969. (PB-185 966)

NESCTM 18 On the Statistical Relation Between Geopotential Height and Temperature-Pressure Profiles. W. L. Smith and S. Fritz, November 1969. (PB-189 276)

NESCTM 19 Applications of Environmental Satellite Data to Oceanography and Hydrology. E. Paul McClain, January 1970. (PB-190 652)

NESCTM 20 Mapping of Geostationary Satellite Pictures - An Operational Experiment. R. C. Doolittle, C. L. Bristor and L. Lauritson, March 1970. (PB-191 189)

NESCTM 21 Reserved.

NESCTM 22 Publications and Final Reports on Contracts and Grants, 1969--NESC. Staff Members, January 1970. (PB-190 632)

NESCTM 23 Estimating Mean Relative Humidity from the Surface to 500 Millibars by use of Satellite Pictures. Frank J. Smigielski and Lee M. Mace, March 1970. (PB-191 741)

NESCTM 24 Operational Brightness Normalization of ATS-1 Cloud Pictures, V. Ray Taylor. (In preparation)

University of Alberta Library
0 1620 0329 3394